Published in final edited form as:
Biomacromolecules. 2008 October ; 9(10): 2863. doi:10.1021/bm800658x.

Hydrogels for Osteochondral Repair Based on Photo-crosslinkable Carbamate Dendrimers

Lovorka Degoricija[†], **Prashant N. Bansal**[†,‡], **Serge H. M. Söntjens**[†], **Neel Joshi**[†], **Masaya Takahashi**[†,§], **Brian Snyder**[‡], and **Mark W. Grinstaff**[†]

[†]Departments of Biomedical Engineering and Chemistry, Boston University, Boston, MA

[‡]Biomechanics Laboratory, Beth Israel Deaconess Medical Center, Boston, MA

[§]Department of Radiology, Beth Israel Deaconess Medical Center, Boston, MA

Abstract

First generation, photo-crosslinkable dendrimers consisting of natural metabolites (i.e. succinic acid, glycerol, and β-alanine) and non-immunogenic poly(ethylene glycol) (PEG) were synthesized divergently in high yields using ester and carbamate forming reactions. Aqueous solutions of these dendrimers were photo-crosslinked with an eosin-based photo-initiator to afford hydrogels. The hydrogels displayed a range of mechanical properties based on their structure, generation size, and concentration in solution. All of the hydrogels showed minimal swelling characteristics. The dendrimer solutions were then photo-crosslinked *in situ* in an *ex vivo* rabbit osteochondral defect (3 mm diameter and 10 mm depth), and the resulting hydrogels were subjected to physiologically relevant dynamic loads. Magnetic resonance imaging (MRI) showed the hydrogels to be fixated in the defect site after the repetitive loading regimen. The ([G1]-PGLBA-MA)$_2$-PEG hydrogel was chosen for the 6 month pilot *in vivo* rabbit study because this hydrogel scaffold could be prepared at low polymer weight (10wt%) and possessed the largest compressive modulus of the 10% formulations, a low swelling ratio, and contained carbamate linkages which are more hydrolytically stable than the ester linkages. The hydrogel treated osteochondral defects showed good attachment in the defect site and histological analysis showed the presence of collagen II and glycosaminoglycans (GAGs) in the treated defects. By contrast, the contralateral unfilled defects showed poor healing and negligible GAG or collagen II production. Good mechanical properties, low swelling, good attachment to the defect site, and positive *in vivo* results illustrate the potential of these dendrimer-based hydrogels as scaffolds for osteochondral defect repair.

Keywords

Osteochondral defects; Cartilage; Tissue Engineering; Scaffolds; Hydrogel; Dendrimer; Dendritic Polymer

---

Osteoarthritis (OA) is the most common form of arthritis, and affects over 20 million people each year.[1] Early treatments include the use of anti-inflammatory drugs and physical therapy to relieve pain and maintain motion. When these methods are no longer effective, they are followed by cartilage grafting to repair discrete chondral lesions and ultimately total joint arthroplasty for advanced arthritis.[2,3] In the initial stages of OA, proteoglycans are lost from the cartilage tissue followed by loss of the collagenous proteins.[2,4] These events lead to formation of small discrete lesions in the cartilage tissue. With disease progression these lesions increase in size and depth, eventually reaching the subchondral bone.[5–7] Next, bone marrow cells migrate to the defect site, affording a healing response consisting of the formation of fibrocartilage.8 Fibrocartilage is mechanically inferior to the native hyaline cartilage, and is thus not as effective for load-bearing at this location. This natural healing response is the basis

for many treatment strategies and surgical techniques to treat discrete osteochondral defects and OA such as abrasion, mosaicoplasty, and microfracture.[9–11] These procedures have seen variable degrees of success, but always lead to the formation of fibrocartilage. An alternative approach is autologous chondrocyte implantation. This cell therapy-based procedure for osteochondral defect repair (Carticel™, Genzyme, Cambridge, MA) is being used in clinics, but it has met with only partial success, especially in treating large size defects of the patellofemoral joint.[12,13] Additional complications such as donor site morbidity and the difficulty of the surgical technique itself limit the utility of this procedure. Thus, there is a clinical need for more effective OA treatments.

Strategies to repair cartilage using tissue engineering typically involve polymer-based scaffolds, cells, and/or growth factors to create the required hyaline cartilage.[2,14–16] The scaffold plays a key role in the repair of osteochondral defects, and must meet a number of criteria; it must: 1) possess similar mechanical properties as the native tissue; 2) support the growth and proliferation of the required local cell phenotype; 3) be a resorbable three-dimensional porous structure; 4) be biocompatible and non-immunogenic *in vivo*; and 5) remain integrated in the defect while subjected to repetitive physiological loads until the tissue repair is complete.

Hydrogels have been used successfully as scaffolds to encapsulate cells in a three dimensional environment.[17–23] The high water content of the scaffold allows for efficient diffusion of nutrients and oxygen in to, and waste and carbon dioxide out of the hydrogel. One example of a hydrogel-based tissue engineering scaffold was prepared from poly(ethylene glycol) diacrylate. This photo-crosslinkable linear polymer can be polymerized *in situ* to form a hydrogel.[24] Hydrogels based on these simple bifunctional PEG diacrylates are able to match the mechanical properties of cartilage at high polymer concentrations, and have shown short-term support for chondrocytes at lower polymer concentrations. However, the efficacy of the PEG diacrylate scaffolds *in vivo* is limited by their excessive swelling after crosslinking and their resistance to timely biodegradation. These materials can swell up to 150%, which is detrimental for any application in a confined defect. The lack of scaffold degradation inhibits the cell growth and the deposition of natural extracellular matrix, decreasing long-term viability. Consequently, PEG-based scaffolds have been modified to degrade *in vivo* by introducing a polylactide segment resulting in a PLA-PEG-PLA diacrylate block co-polymer. The photocrosslinked PLA-PEG-PLA scaffolds support cellular proliferation, but are limited by non-optimal mechanical properties. Anseth *et al*. have also reported scaffolds based on polyvinyl alcohol and polyesters that allow for biodegradation.[25] An elegant approach was reported by Hubbell and coworkers who prepared a scaffold possessing a peptide sequence cleavable by enzymes (e.g., fibrinogen) and a linear PEG diacrylate.[26] This work was extended to the use of crosslinkable 4- and 8- arm PEG-based hydrogels with a peptide sequence susceptible to matrix metalloproteinase degradation for encapsulation of primary bovine calf chondrocytes.27

Two important design criteria for these *in situ* photocrosslinkable polymers are effective delivery to a defect site and the resulting formation of a crosslinked hydrogel. We believe that a biocompatible polymer containing multiple crosslinking sites is an ideal macromer for cartilage defect repair, because this approach allows for an increase in the crosslink density of the gel without significantly increasing the polymer concentration. This approach affords improved mechanical properties and reduced swelling while maintaining degradable sites such as ester linkages. Dendrimers—highly branched and regularly structured macromolecules—offer a number of important advantages for scaffold optimization over linear or branched polymers. Specifically, dendrimers exhibit low solution viscosities, high solubility, narrow molecular weight distributions, and multiple end groups for functionalization.[28–36] Additionally, the synthesis and the choice of monomers is highly flexible, since these

macromolecules are synthesized in a repetitive manner by either a convergent or divergent approach. Our current focus is on dendritic macromolecules composed of natural metabolites (*i.e.*, succinic acid, glycerol, and ß-alanine) connected to a non-immunogenic poly(ethylene glycol) core by ester and/or carbamate functionalities in an ABA-type architecture,[37] as shown schematically in figure 1. These new macromolecules belong to a family of dendritic polymers which we are investigating for drug delivery,[38–41] corneal wound repair,[42–48] and tissue engineering applications.[21,49–54] We have previously reported a polyester-PEG dendritic linear copolymer for preparing hydrogel scaffolds and the resulting hydrogel supported chondrocytes and the production of extracellular matrix such as GAG and collagen type II *in vitro*.[21]

Most cartilage tissue engineering strategies attempt to use a cell-encapsulated polymer-based scaffold to grow the desired tissue *in vitro*, and then implant the healthy tissue into the defect site of the patient. Our interest is in evaluating whether a scaffold alone can have a positive outcome on repair of osteochondral defects. To this end, we designed and synthesized four different biocompatible photocrosslinkable dendrimer-PEG-dendrimer block co-polymers and evaluated their mechanical properties after crosslinking and hydrogel formation. One hydrogel formulation was chosen based on its mechanical similarity to native articular cartilage, low swelling properties, and macrofixation to the defect site and evaluated in a pilot *in vivo* study of osteochondral defect repair. This approach offers several advantages over other cartilage tissue engineering methods in that it requires no cell implantation and will simplify surgical procedures through the use of an injectable polymer solution that can be photocrosslinked *in situ*.

Experimental Section

For complete details on the syntheses, characterization, hydrogel preparation, rheological measurements, hydrogel swelling, dynamic mechanical testing for tissue integration, magnetic resonance imaging (MRI), and pilot *in vivo* studies, please see the supporting information document.

Results

The four dendritic macromolecules with varying layers of carbamate and ester linkages under investigation are shown in Figure 2. The poly(glycerol succinic acid) and poly(glycerol beta-alanine) units are denoted as PGLSA and PGLBA, respectively, and polyethylene glycol is denoted as PEG, while the zeroth and first generations are denoted as [G0] and [G1]. Thus, the abbreviated names for the dendritic macromolecules are: **([G0]-PGLBA-[G1]-PGLSA**-OH)$_2$-**PEG**, (**[G1]-PGLBA**-OH)$_2$-**PEG**, (**[G0]-PGLSA-[G1]-PGLBA**-OH)$_2$-**PEG**, and (**[G1]-PGLSA**-OH)$_2$-**PEG**.

To prepare the generation one (**([G0]-PGLBA-[G1]-PGLSA**-OH)$_2$-**PEG**) macromolecule, PEG (average Mw of 3400) was reacted with 4 eq of **1** (see SI for preparation) in DCM with a catalytic amount of dibutly tindilaruate (DBTDL). This afforded the zeroth generation (G0) carbamate benzyl protected (bn) PEG dendrimer, **2 ([G0]-PGLBA**-bn)$_2$-**PEG**), in 89% yield. This was followed by a hydrogenolysis reaction in THF with 10% wt Pd/C catalyst to afford the deprotected zeroth generation carbamate PEG dendrimer, **([G0]-PGLBA**-OH)$_2$-**PEG**), **3**, in quantitative yield. An esterification reaction with 8 eq of PGLSA anhydride, **4**, coupled to **3** in pyridine gave the benzylidine protected (bzld) first generation carbamate-ester PEG dendrimer, (**([G0]-PGLBA-[G1]-PGLSA**-bzld)$_2$-**PEG**, **5**, in 91% yield. The benzylidene acetal group was cleaved by a hydrogenolysis reaction in THF in the presence of a Pd/C catalyst. The deprotected (OH) first generation carbamate-ester PEG dendrimer, **([G0]-PGLBA-[G1]-PGLSA**-OH) $_2$-**PEG**, **6**, was obtained in quantitative yield, figure 3a.

The carbamate-linked (**[G1]-PGLBA-OH**)$_2$-**PEG** dendritic copolymer was synthesized by reacting 8 eq of **1** with **3** in DCM with a catalytic amount of DBTDL (Figure 2b). The benzyl protected first generation carbamate-carbamate PEG dendrimer, (**[G0]-PGLBA-bn**)$_2$-**PEG**)$_2$-PEG, **8**, was obtained in 80% yield. Next, a hydrogenolysis reaction in the presence of Pd/C catalyst in THF was used to cleave the benzyl protecting groups. This afforded the deprotected first generation poly(glycerol beta-alanine)-PEG dendritic copolymer, (**[G1]-PGLBA-OH**)$_2$-**PEG**, **9**, in near quantitative yield, figure 3b.

Next, the ester-carbamate linked (**[G0]-PGLSA-[G1]-PGLBA**-OH)$_2$-**PEG** dendrimer was obtained by coupling 4 eq of the activated PGLSA anhydride, **4**, with PEG, in pyridine, to afford the benzylidene protected zeroth generation ester PEG dendrimer, ((**[G0]-PGLSA**-bzld)$_2$-**PEG**, **11**, in 96% yield. A hydrogenolysis reaction with 10% wt Pd/C catalyst was used to cleave the benzylidene acetal protecting group in near quantitative yield to afford the deprotected zeroth generation ester PEG dendrimer, (**[G0]-PGLSA**-OH)$_2$-PEG, **12**. Next, a condensation reaction of **12** with 8 eq of **1** in DCM and a catalytic amount of DBTDL afforded the benzyl protected first generation ester-carbamate PEG dendrimer, (**[G0]-PGLSA-[G1]-PGLBA**-bn)$_2$-**PEG**, **13**, in 83% yield. Lastly, a hydrogenolysis reaction afforded the deprotected first generation ester-carbamate PEG dendrimer, (**[G0]-PGLSA-[G1]-PGLBA**-OH)$_2$-**PEG**, **14**, in near quantitative yield, figure 3c.

The (**[G1]-PGLSA**-OH)$_2$-**PEG dendrimer** was synthesized using a similar approach of iterative couplings with the activated PGLSA monomer followed by deprotection reactions, as previously described by Carnahan et al.[43] All of the esterification and condensation reactions were precipitated twice in cold ether and the hydrogenolysis reactions were precipitated once in cold ether.

For all formulations, the hydroxy periphery of the first generation dendrimers was modified with methacrylate groups. This was performed by coupling 16 eq of methacrylic anhydride to **7**, **10**, **15**, and the (**[G1]-PGLSA**-OH)$_2$-**PEG** in pyridine at 0 °C, affording the methacrylated (MA) first generation PEG dendrimers, **([G0]-PGLBA-[G1]-PGLSA**-MA)$_2$-**PEG**, **7**, (**[G1]-PGLBA**-MA)$_2$-**PEG**, **10**, (**[G0]-PGLSA-[G1]-PGLBA**-MA)$_2$-**PEG**, **15**, and (**[G1]-PGLSA**-MA)$_2$-**PEG**, figure 2 (a–c). The methacrylation reactions were precipitated twice in cold ether to yield white powders in 75 – 87% yield.

Hydrogel Preparation—The dendritic macromers were dissolved in aqueous PBS solution at 5, 10, or 20 wt % and photo-crosslinked with an Argon-ion laser. Specifically, the methacrylated dendritic formulations (**([G0]-PGLBA-[G1]-PGLSA**-MA)$_2$-**PEG**, **7**, (**[G1]-PGLBA**-MA)$_2$-**PEG**, **10**, (**[G0]-PGLSA-[G1]-PGLBA**-MA)$_2$-**PEG**, **15**, and (**[G1]-PGLSA**-MA)$_2$-**PEG**) were dissolved in PBS followed by the addition of the eosin-Y based photo-initiator system. Next, 160 μL of this dendrimer solution was placed in a cylindrical mold and photo-crosslinked with an argon ion laser for 120 seconds (514 nm, 200 mW). The hydrogel was soft, smooth, pliable and adhesive to the touch.

Hydrogel Swelling—The swelling characteristics of the four groups of hydrogel scaffolds were evaluated at concentrations of 5, 10, and 20% w/v. Most of the formulations exhibited minimal swelling over the 30 days. An initial increase in swelling was observed at 15 days incubation time for the 10% w/v **([G0]-PGLBA-[G1]-PGLSA**-MA**)$_2$-PEG**, and **([G0]-PGLSA-[G1]-PGLBA**-MA**)$_2$-PEG**, and 20% w/v **([G0]-PGLBA-[G1]-PGLSA**-MA**)$_2$-PEG**, and **([G1]-PGLSA**-MA**)$_2$-PEG**, hydrogels (Figure 4). These macromolecules show a 27%, 24%, 13%, and 12% increase in swelling after 30 days incubation, respectively. The 5 through 10% w/v **([G1]-PGLSA**-MA**)$_2$-PEG**, and 5 through 20% w/v **([G1]-PGLBA**-MA**)$_2$-PEG** hydrogels showed no significant swelling. Likewise, the 5, and 20% w/v **([G0]-PGLSA-[G1]-PGLBA**-MA**)$_2$-PEG**, and 5% w/v **([G0]-PGLBA-[G1]-PGLSA**-MA**)$_2$-PEG** hydrogels

also showed minimum swelling during the 30 day swelling study. The 10 and 20% w/v **[G0]-PGLBA-[G1]-PGLSA**-MA)$_2$**-PEG**, 20% w/v **([G1]-PGLSA**-MA)$_2$**-PEG** and 20% w/v ([G1]-CC-MA)$_2$-PEG formulations swelled the most, with swelling ratios of 27%, 13%, 12%, and 6%, respectively.

Rheological measurements—The mechanical properties of each hydrogel were measured for all four dendrimer formulations over a range of concentrations (5, 10, and 20% w/v) before and after swelling (Figure 5). The mechanical properties showed high concentration dependence for all four formulations with the higher polymer concentrations affording stiffer materials. The compressive and complex shear modulus increased with increasing macromolecular concentration for the hydrogels before swelling and the loss angle decreased. After swelling, the compressive and shear modulus decreased for all concentrations and the loss angle increased while the trends were preserved for all the above parameters. The specific values for the mechanical properties of the hydrogels can be found in Table 1 for before swelling and Table 2 for after swelling.

Dynamic mechanical testing for evaluating the macro-fixation of the hydrogel in a simulated osteochondral defect—The macro-fixation of the hydrogels in a confined defect was evaluated using an *ex vivo* rabbit knee model. A description of the method and a figure showing the set-up can be found in the SI. After photocrosslinking in the simulated osteochondral defect, the scaffolds were subjected to dynamic mechanical loading (300 cycles) with a physiologically relevant load (30 N at the end of the tibia simulating the body weight of a 3 kg rabbit). The dead weight was selected based on evidence that a ground reaction force of approximately one times body weight acts at the rabbit foot during hopping.[55] Upon completion of the loading regimen, all four formulations at 5, 10, and 20% w/v remained intact in the defect site when visually inspected. Magnetic resonance imaging (MRI) was performed for all the formulations to qualitatively evaluate the fixation between the hydrogel and the hydrogel-bone interface. Representative MR images of the medial femoral condyle show that the 5, 10, and 20% w/v (**[G1]-PGLBA**-MA)$_2$**-PEG** hydrogels completely fill the entire volume of the defect after loading (Figure 6). Similar results were observed with all of the other formulations. These results highlight the advantage of using a solution phase-to-gel system that forms *in situ* to completely fill a defect shape compared to preformed materials, which usually require suture-based fixation or have to be press fitted into the irregularly shaped defect.

Pilot *in vivo* studies—The 10% (w/v) (**[G1]-PGLBA**-MA)$_2$**-PEG** hydrogel formulation was chosen for use in an *in vivo* study based on several criteria. While the 20% (w/v) hydrogels exhibited higher mechanical resilience, previous work in our lab with similar dendritic architectures has shown that hydrogels made from dendrimer concentrations greater than 10% (w/v) do not allow for cell proliferation *in vitro*.[21] Of the four different 10% (w/v) dendrimer hydrogels, (**[G1]-PGBLA**-MA)$_2$-PEG had the largest compressive modulus of the formulations, low swelling characteristics, and high water content (90 wt%).

Three New Zealand white rabbits (Male, 24 weeks) were subjected to surgery to introduce full-thickness osteochondral defects (3 mm diameter and 10 mm depth) in both of their medial femoral condyles. One defect in each rabbit was left unfilled to serve as an internal control. In the contralateral knee, the bone marrow that initially filled the defect was first aspirated out, then the dendrimer solution was injected and photocrosslinked *in situ* immediately to yield a hydrogel. After the surgery was complete, the rabbits were allowed free cage activity during the course of the experiment.

After 24 weeks, the rabbits were sacrificed and the knees were fixed in formalin, decalcified and subjected to histological analysis to determine cellularity (H&E stain), GAG (Safranin-O stain) and collagen (Masson's trichrome) synthesis (Figure 7). The samples were also subjected

to immunohistochemical analysis to determine the type of collagen in each defect. The healing response in the scaffold-filled knees exhibited significant staining for collagen II and GAG, indicating the presence of hyaline-like cartilage. By contrast, the unfilled controls appeared to be filled irregularly and showed minimal GAG production. The unfilled defects stained slightly for collagen I, but did not show any staining for collagen II. Digital pictures of the femurs after sacrifice also show a much smoother cartilage surface for the filled defects.

Discussion

Photocrosslinkable dendrimers were synthesized divergently, using an iterative approach involving a combination of coupling and deprotection steps to prepare higher generation macromolecules. This synthetic route exhibited several attractive features. The ester- and carbamate-forming reactions that were used to introduce branching proceeded with high yields (> 91% and > 83%, respectively), and the hydrogenolysis deprotection steps usually proceeded quantitatively. Additionally, the purification at each step was minimal, since the presence of the 3400 Da PEG core allowed for precipitation of the desired product in cold diethyl ether after each synthetic step.

Importantly, after capping the terminal hydroxyl groups with methacrylate moieties, the resulting dendrimers were water soluble, and could be crosslinked to form hydrogels using a mild and facile photochemical procedure. This system had the additional benefits that make it amenable to future *in vivo* clinical applications. The vividly pink color of eosin in the hydrogel was easily observed when placed in the defect site facilitating efficient filling. The photocrosslinking process required about two minutes using this photopolymerization set-up.

One of the main advantages of dendrimer scaffolds for cartilage repair is the ability to tune the mechanical properties of the resulting hydrogels by altering the dendritic structure. Rheological analysis of these 12 different hydrogel formulations (4 dendrimer structures and 3 concentrations) showed that they exhibited a range of values for compressive modulus, complex shear modulus, and loss angle. These parameters are relevant to cartilage biomechanics in that they respectively indicate the compressive stiffness, shear resistance, and viscoelasticity of the hydrogels. Several trends in mechanical properties of the hydrogel scaffolds were observed throughout the course of this study: 1) the E and |G*| increased as the weight percent of the polymer increased for all four formulations resulting in a stiffer material in shear and compression, equally important for cartilage tissue engineering scaffolds; 2) the δ decreased as the weight percent of the polymer increased from 5 to 20% w/v, indicating a more elastic material: 3) the same E, |G*| and δ were observed for the **([G0]-PGLSA-[G1]-PGLBA-**MA**)$_2$-PEG** and **([G0]-PGLBA-[G1]-PGLSA-**MA**)$_2$-PEG**, which indicated that the order of the carbamate linkage did not affect the overall mechanics; 4) the **([G1]-PGLSA-**MA**)$_2$-PEG** had similar E, |G*| and δ to **([G0]-PGLSA-[G1]-PGLBA-**MA**)$_2$-PEG** and **([G0]-PGLBA-[G1]-PGLSA-**MA**)$_2$-PEG** at 5 and 10% w/v; 5) the **([G1]-PGLBA-**MA**)$_2$-PEG** had the highest E and |G*| and the lowest δ at 20% w/v, indicating a more elastic and resilient material as compared to the other formulations; 6) as the hydrogels reached their equilibrium swelling, there was an overall decrease in the E, |G*| and δ by 50%. The most resilient formulation was the 20 w/v% preparation with the **([G1]-PGLBA-MA$_2$)-PEG** dendrimer, which displayed a compressive modulus of ~700 kPa, on par with the lower limit of articular cartilage (700–1300 kPa). The loss angle for this formulation was 3°, indicating a highly elastic material, comparable to the normal range of articular cartilage elasticity. Although the shear modulus was affected by the structure and concentration of the dendrimer, the highest values obtained were three times lower than those for native articular cartilage. These results showed that the scaffolds partially fulfill the mechanical requirements for an effective temporary cartilage surrogate.

Since defects resulting from osteoarthritis or trauma are generally irregular in shape and confined in geometry, placement and fixation of the scaffold in the site are important for optimal performance. Yet, many current approaches to cartilage repair utilize scaffolds that must be press-fit or sutured into the defect site, potentially causing additional trauma to the surrounding healthy cartilage. Consequently, scaffolds that can be injected into the wound site as an aqueous solution and then crosslinked *in situ* to conform to the size and shape of the defect are especially attractive. For these types of scaffolds, swelling of the hydrogel is a key concern in evaluating the potential efficacy of these scaffolds. In our studies, the lower weight percent formulations showed the least amount of swelling, while the 20 w/v% formulations swelled by as much as 25%. We also found, as expected, that swelling reduced the mechanical properties of the hydrogels. The multivalent nature of the dendritic macromolecules provided multiple crosslinking sites per macromolecule, which upon hydrogel formation resulted in scaffolds with low swelling characteristics. By comparison, many purely PEG-based hydrogels exhibit considerable swelling by water uptake, hindering their utility in an *in vivo* setting.

To address the fixation of hydrogel scaffolds into an actual defect site, we introduced osteochondral defects into excised rabbit knees, filled the defect with the aqueous solution containing the dendritic crosslinkable macromer, and photocrosslinked the solution *in situ* to form the scaffold. As expected, the resulting hydrogels conformed to the size and shape of the defect. After repetitive mechanical loading of the joint with physiologically relevant forces, MR images showed that all of the hydrogel formulations completely filled the volume of the defect and remained fixed in the defect.

The 6-month pilot *in vivo* study was undertaken to evaluate procedural issues during surgery and performance of the hydrogel scaffolds in a full-thickness osteochondral defect. We elected to use the carbamate-ester-ether ((**[G1]-PGLBA**-MA)$_2$**-PEG)** hydrogel scaffold at 10 w/v % based on its low swelling and high compressive and dynamic shear modulus. Also, in previous *in vitro* cell proliferation experiments with similar poly(ester) based dendrimers, extensive cell proliferation and production of GAG and collagen II was observed. In those studies, the hydrogel was degraded within three to four weeks.[21] The pilot study described in this paper revealed that the carbamate-ester-ether base hydrogel was well tolerated by the animals and remained fixed and intact in the defect site during the course of the experiment. Histological analysis of the knees after sacrifice revealed that the treated knees had strong staining for collagen II and GAG. By comparison, the untreated defects showed only collagen I production and very little GAG production. At this point, the source of the cells responsible for the healing response in the filled defects is unclear. It is likely that that cells from both the marrow and the surrounding tissues replaced the hydrogel as it was being degraded. Importantly, the histological data shows that the healing response in the filled defects looks qualitatively more promising than that in the unfilled defects. It is also noteworthy to mention that the *in situ* photocrosslinking technique employed is amenable to arthroscopic procedures, and therefore may be easily translated to the clinic.

Conclusion

The new PEG-core crosslinkable dendrimers reported herein display several attractive features for cartilage tissue repair. The dendritic macromolecules are synthesized in a high yielding, facile, and divergent manner, whereby the linkages within the polymer structure are varied from one generation to another. The carbamate-linked dendrimer based hydrogels rival the compressive stiffness and viscoelasticity of native articular cartilage. Upon photocrosslinking the injected macromer solution in an osteochondral defect, the dendrimer hydrogels conform to fit the size and shape of the defect and remain fixed in the defect site even after repetitive mechanical loading. The pilot *in vivo* study showed that even without the use of implanted cells, these hydrogel scaffolds induce a positive healing response in the form of cell infiltration

and GAG and collagen II production. Several questions remain about the mechanism of the observed healing: which cells were responsible, how did they infiltrate the matrix, and how were they stimulated to produce ECM containing collagen II. These questions will be addressed in future experiments. Ongoing studies will also explore the use of scaffolds that are spatially differentiated to match the properties of the stratified bone and cartilage tissues.

The successful use of dendrimer based hydrogel scaffolds in the above osteochondral defect models demonstrates the potential of these materials for further *in vivo* applications. These highly branched well-defined macromolecules offer a number of opportunities to control the structure, and optimize the macromolecular properties and the resulting hydrogels. As such hydrogels prepared from dendritic macromolecules – be it the polymers described herein or other systems - are of interest and should be pursued further for cartilage tissue engineering. The clinical solution will likely require a scaffold material that is compatible with (autologous) chondrocytes, promotes or retains the correct cell phenotype, efficiently fills and integrates well with the defect site, supports the relevant physiological loads, and is easily administered to the site, preferably by a non-invasive surgical technique. These hydrogels fulfill many of these requirements and hence are exciting prospects for additional *in vitro* and *in vivo* evaluation. Continued basic and clinical research in this area will lead to new materials, procedures, and strategies for the repair of articular cartilage defects.

Supplementary Material

Refer to Web version on PubMed Central for supplementary material.

Acknowledgments

These studies were funded in part by the BU and the NIH. SHMS thanks the Netherlands Organization for Scientific Research (NWO) for a Talent scholarship.

References

1. 2007 www.arthritis.org.
2. Hunziker EB. Osteoarthritis and Cartilage Osteoarthritis Cartilage 2002;10:432–463.
3. Chen FS, Frenkel SR, Di Cesare PE. Am J Orthop 1999;28:88–96. [PubMed: 10067711]
4. Mow, VC.; Ratcliffe, A. Structure and Function of Articular Cartilage and Meniscus. 2nd ed.. Philadelphia: Lippincott Raven; 1997.
5. Goldring MB. Arthritis Rheum 2000;43:1916–1926. [PubMed: 11014341]
6. Simon L. Clin Cornerstone 1999;2:26–37. [PubMed: 10689542]
7. Felson D. Rheum Dis Clin North Am 1993;19:607–615. [PubMed: 8210577]
8. Furukawa T, Eyre DR, Koide S, Glimcher MJ. J Bone Joint Surg 1980;62A:79–89. [PubMed: 7351420]
9. Akizuki S, Yasukawa Y, Takizawa T. Arthroscopy 1997;13:9–17. [PubMed: 9043599]
10. Belvins FT, Steadman JR, Rodrigo JJ, Silliman J. Orthopedics 1998;21:761–767. [PubMed: 9672913]
11. Ghivizzsani SC, Oligino TJ, Robbins PD, Evans CH. Phys. Med. Rehab. Clin. North Am 2000;11:289–307.
12. Brittberg M, Lindahl A, Nilsson A, Ohlsson C, Isaksson O, Peterson L. New England Journal of Medicine 1994;331:889–895. [PubMed: 8078550]
13. Richardson JB, Caterson B, Evans EH, Ashton BA, Roberts S. J Bone Joint Surg Br 1999;81:1064–1068. [PubMed: 10615987]
14. Temenoff JS, Mikos AG. Biomaterials 2000;21:431–440. [PubMed: 10674807]
15. Freed LE, Guilak F, Guo XE, Gray ML, Tranquillo R, Holmes JW, Radisic M, Sefton MV, Kaplan D, Vunjak-Novakovic G. Tissue Eng 2006;12:3285–3305. [PubMed: 17518670]
16. Schaefer D, Martin I, Jundt G, Seidel J, Heberer M, Grodzinsky A, Bergin I, Vunjak-Novakovic G, Freed LE. Arthritis and Rheumatism Arthritis Rheum 2002;46:2524–2534.

17. Freed LE, Marquis JC, Nohria A, Emmanual J, Mikos AG, Langer R. J. Biomed. Mat. Res 1993;27:11–23.
18. Hauselmann HJ, Fernandes RJ, Mok SS, Schmid TM, Block JA, Aydelotte MB, Kuettner KE, Thonar EJ. J Cell Sci 1994;107:17–27. [PubMed: 8175906]
19. Grande DA, Halberstadt C, Naughton G, Schwartz R, Manji R. J Biomed Mater Res 1997;34:211–220. [PubMed: 9029301]
20. Sims CD, Butler PE, Casanova R, Lee BT, Randolph MA, Lee WP, Vacanti CA, Yaremchuk MJ. Plast Reconstr Surg 1996;98:843–850. [PubMed: 8823024]
21. Söntjens SHM, Nettles DL, Carnahan MA, Setton LA, Grinstaff MW. Biomacromolecules 2006;7:310–316. [PubMed: 16398530]
22. Peppas NA, Huang Y, Torres-Lugo M, Ward JH, Zhang J. Annu. Rev. Biomed. Eng 2000;2:9–29. [PubMed: 11701505]
23. Nguyen KT, West JL. Biomaterials 2002;23:4307–4314. [PubMed: 12219820]
24. Elisseeff J, Anseth K, Sims D, McIntosh W, Randolph MA, Yaremchuk M, Langer R. Plastic and Reconstructive Surgery 1999;104:1014–1022. [PubMed: 10654741]
25. Bryant SJ, Anseth KS. J Biomed Mater Res 2003;64A:70–79.
26. Halstenberg S, Panitch A, Rizzi S, Hall H, Hubbell JA. Biomacromolecules 2002;3:710–723. [PubMed: 12099815]
27. Park Y, Lutolf MP, Hubbell JA, Hunziker EB, Wong M. Tissue Engineering 2004;10:515–522. [PubMed: 15165468]
28. Newkome GR, Shreiner CD. Polymer 2008;49:1–173.
29. Tomalia, DA.; Fréchet, JMJ. Dendrimers and Other Dendritic Polymers. ed.. Chichester: Wiley and Sons Ltd; 2001. p
30. Tomalia DA. Prog. Polym. Sci 2005;30:294–324.
31. Zeng F, Zimmerman SC. Chem. Rev 1997;97:1681–1712. [PubMed: 11851463]
32. Fischer M, Vogtle F. Angew. Chem. Int. Ed 1999;38:884–905.
33. Grayson SM, Fréchet JMJ. Chem. Rev 2001;101:3819–3868. [PubMed: 11740922]
34. Fréchet, JMJ.; Hawker, CJ. Synthesis and Properties of Dendrimers and Hyperbranched Polymers. ed.. Oxford: Pergamon; 1996.
35. Newkome, GR.; Moorefield, CN.; Vogtle, F. Dendritic Molecules: Concepts, Syntheses, Perspectives. ed.. New York: VCH; 1996.
36. Bosman AW, Janssen HM, Meijer EW. Chem. Rev 1999;99:1665–1688. [PubMed: 11849007]
37. Yin R, Zhu Y, Tomalia DA. J Am Chem Soc 1998;120:2678–2679.
38. Morgan MT, Nakanishi Y, Kroll DJ, Griset AP, Carnahan MA, Wathier M, Oberlies NH, Manikumar G, Wani MC, Grinstaff MW. Cancer Research 2006;66:11913–11921. [PubMed: 17178889]
39. Morgan MT, Carnahan MA, Finkelstein S, Prata CA, Degoricija L, Lee SJ, Grinstaff MW. Chem Commun 2005:4309–4311.
40. Morgan MT, Carnahan MA, Immoos CE, Ribeiro AA, Finkelstein S, Lee SJ, Grinstaff MW. J. Am. Chem. Soc 2003;125:15485–15489. [PubMed: 14664594]
41. Wolinsky JB, Grinstaff MW. Adv. Drug Deliv. Rev 2008;60:1037–1055. [PubMed: 18448187]
42. Grinstaff MW. Biomaterials 2007;28:5205–5214. [PubMed: 17889330]
43. Carnahan MA, Middleton C, Kim J, Kim T, Grinstaff MW. J. Am. Chem. Soc 2002;124:5291–5293. [PubMed: 11996569]
44. Velazquez AJ, Carnahan MA, Kristinsson J, Stinnett S, Grinstaff MW, Kim T. Arch Ophthalmol 2004;122:867–870. [PubMed: 15197062]
45. Wathier M, Jung PJ, Carnahan MA, Kim T, Grinstaff MW. J. Am. Chem. Soc 2004;126:12744–12745. [PubMed: 15469247]
46. Wathier M, Johnson SM, Kim T, Grinstaff MW. Bioconjugate Chem 2006;17:873–876.
47. Degoricija L, Johnson CS, Wathier M, Kim T, Grinstaff MW. IOVS 2007;48
48. Oelker AM, Grinstaff MW. J. Mat. Chem 2008;18:2521–2536.
49. Grinstaff MW. Chem. Eur. J 2002;8:2838–2846.

50. Carnahan MA, Grinstaff MW. Macromolecules 2001;34:7648–7655.
51. Luman NR, Smeds KA, Grinstaff MW. Chem. Eur. J 2003;9:5618–5626.
52. Luman NR, Grinstaff MW. Org. Lett 2005;7:4863–4866. [PubMed: 16235908]
53. Luman NR, Kim T, Grinstaff MW. Pure App. Chem 2004;76:1375–1385.
54. Degoricija L, Carnahan MA, Johnson CS, Kim T, Grinstaff MW. Macromolecules 2006;39:8952–8958.
55. Gushue DL, Houck J, Lerner AL. J Orthop Res 2005;23:735–742. [PubMed: 16022984]

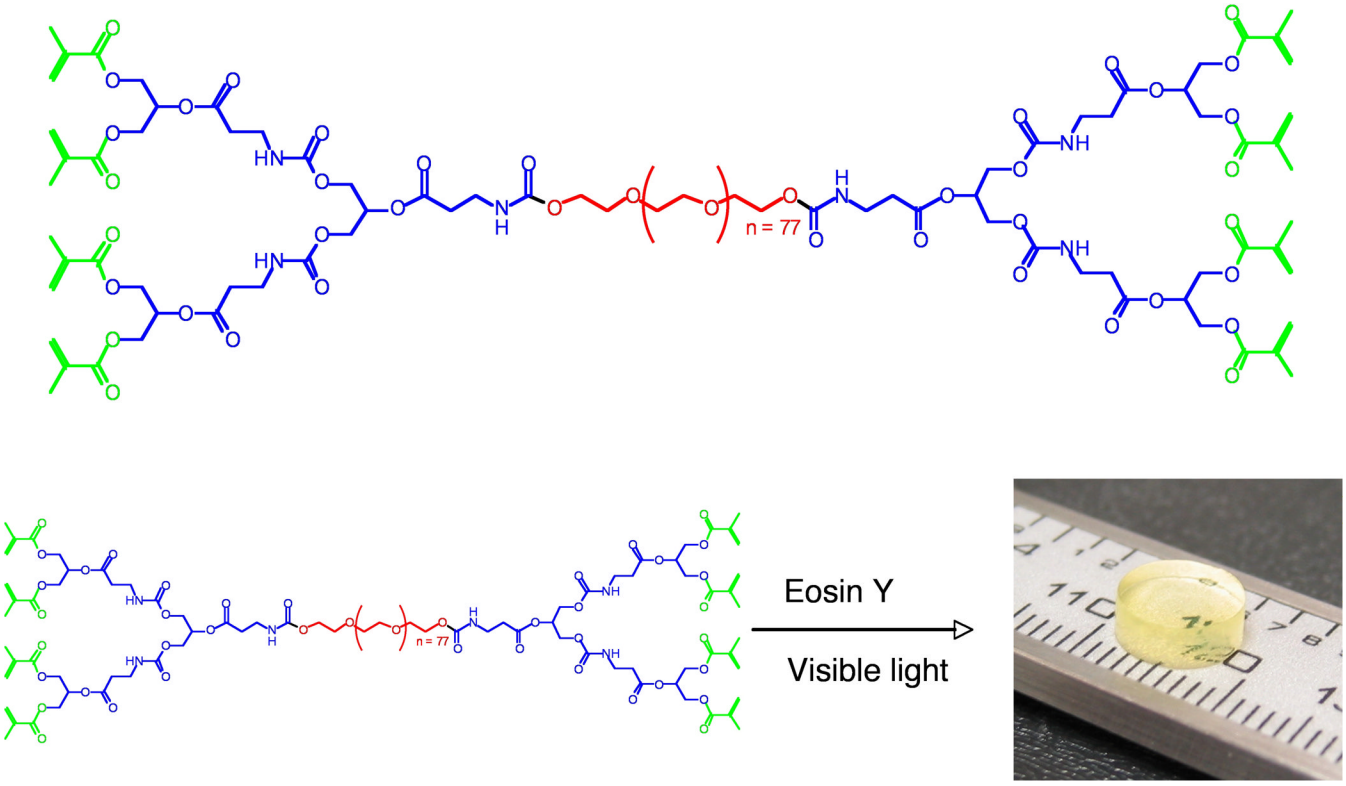

Figure 1.

(top) Drawing of one of the dendrimer macromers used in the study to prepare hydrogel scaffolds. It has an ABA triblock architecture consisting of the A – dendritic part and B –linear PEG part. Here, the dendritic wedges of glycerol and succinic acid or β-alanine are shown in blue, the PEG is shown in red, and the crosslinkbale methacrylate groups shown in green. **(bottom)** The photopolymerization reaction of (**[G1]-PGLBA**-MA)$_2$-**PEG** dendrimer to form a hydrogel which includes the use of an eosin Y photo-initiator and triethanolamine and 1-vinyl-2-pyrrolidinone, as catalyst and co-catalyst, respectively.

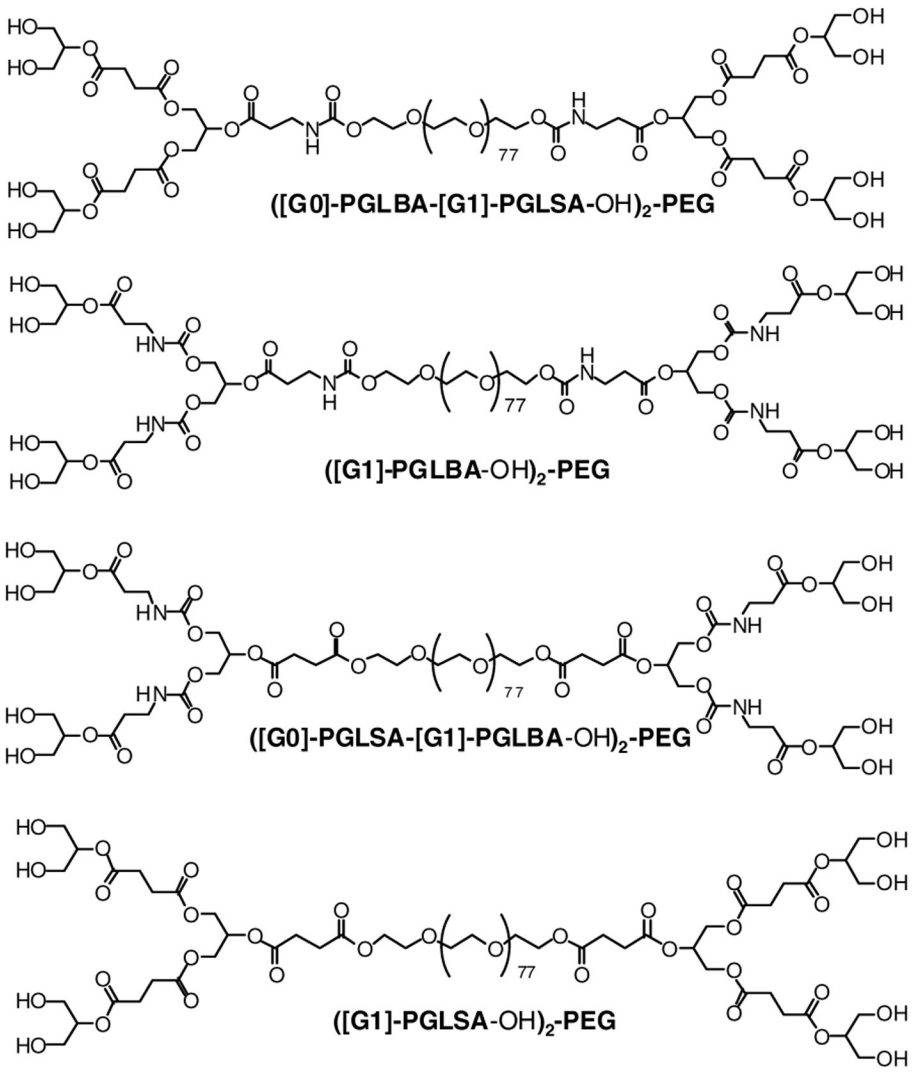

Figure 2.

The structures of the poly(glycerol succinic acid)-co-poly(glycerol beta-alanine) - PEG macromolecules, poly(glycerol beta-alanine)-PEG macromolecule, and poly(glycerol succinic acid)-PEG macromolecule. From top to bottom the structures are: **([G0]-PGLBA-[G1]-PGLSA**-OH)$_2$-**PEG**, (**[G1]-PGLBA-OH**)$_2$-**PEG**, (**[G0]-PGLSA-[G1]-PGLBA**-OH)$_2$-**PEG**, and (**[G1]-PGLSA**-OH)$_2$-**PEG**. A PEG of average Mw 3400 was used and hence n ≈ 77.

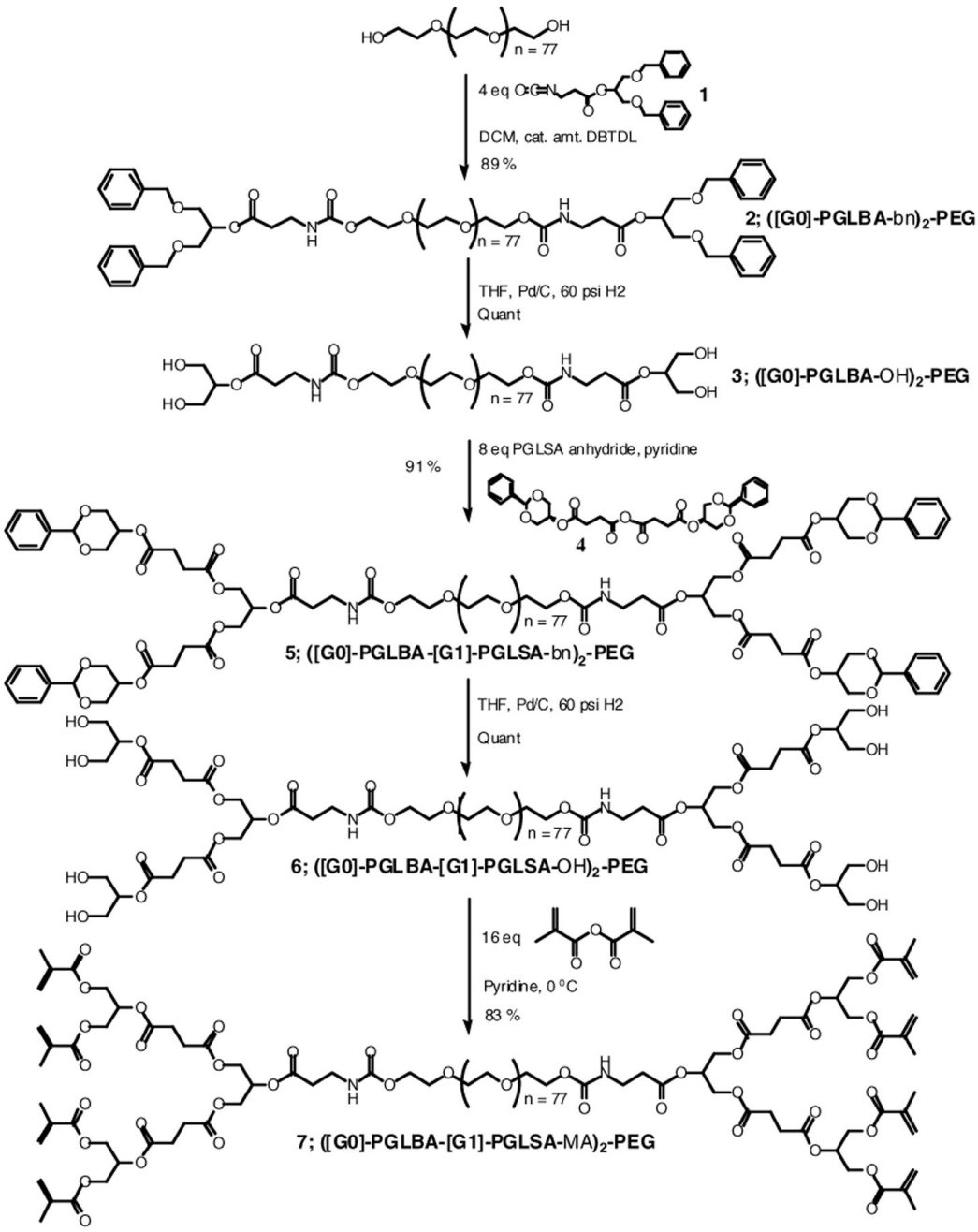

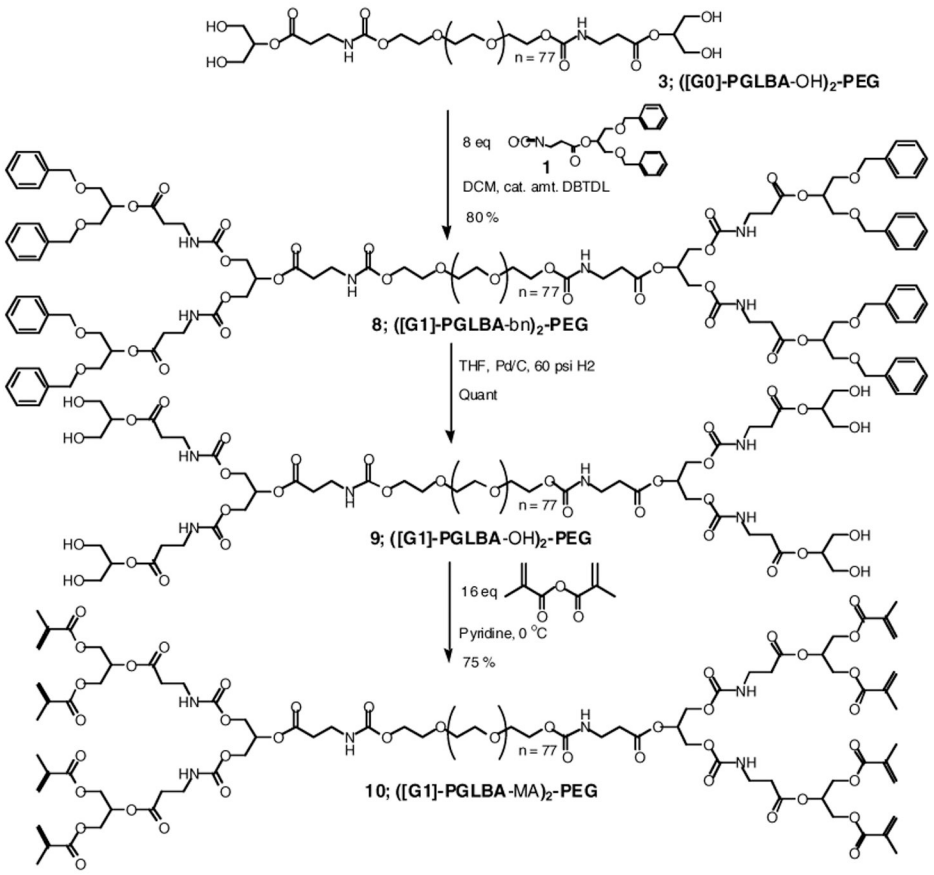

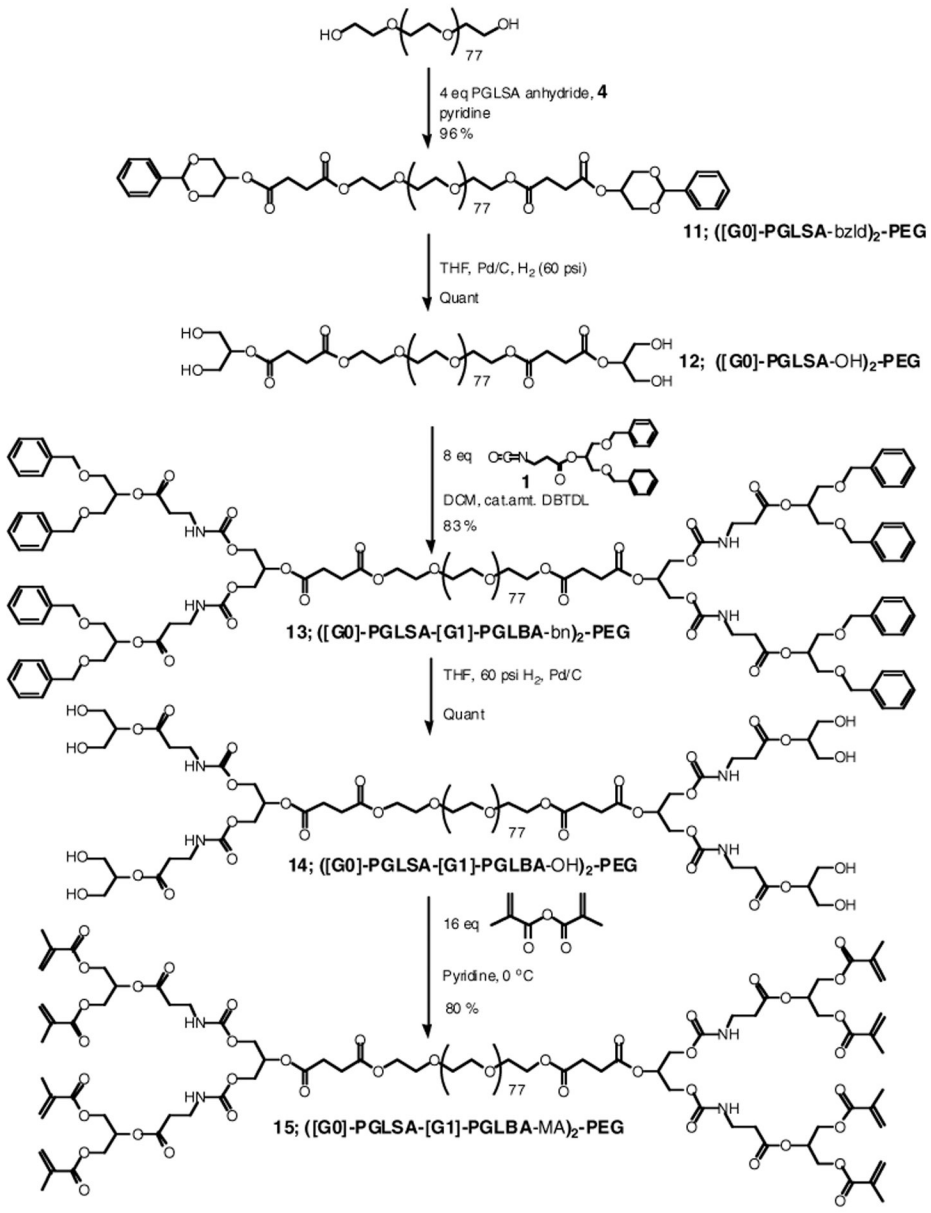

Figure 3.

Figure 3a. The divergent synthesis of (**[G0]-PGLSA-[G1]-PGLBA**-MA)$_2$-**PEG** dendrimers, where n ≈ 77 for a PEG of average Mw 3400. All esterification and condensation reactions proceeded in 83 – 91 % yield. All hydrogenolysis reacting proceeded in near quantitative yield

Figure 3b. The divergent synthesis of (**[G1]- PGLBA-MA**)$_2$-**PEG** dendrimers, where n ≈ 77 for a PEG of average Mw 3400. All esterification and condensation reactions proceeded in 75 – 80 % yield. All hydrogenolysis reactions proceeded in near quantitative yield.

Figure 3c. The divergent synthesis of **([G0]-PGLBA-[G1]-PGLSA**-OH)$_2$-**PEG** dendrimers, where n ≈ 77 for a PEG of average Mw 3400. All esterification and condensation reactions proceeded in 80 – 96 % yield. All hydrogenolysis reactions proceeded in near quantitative yield.

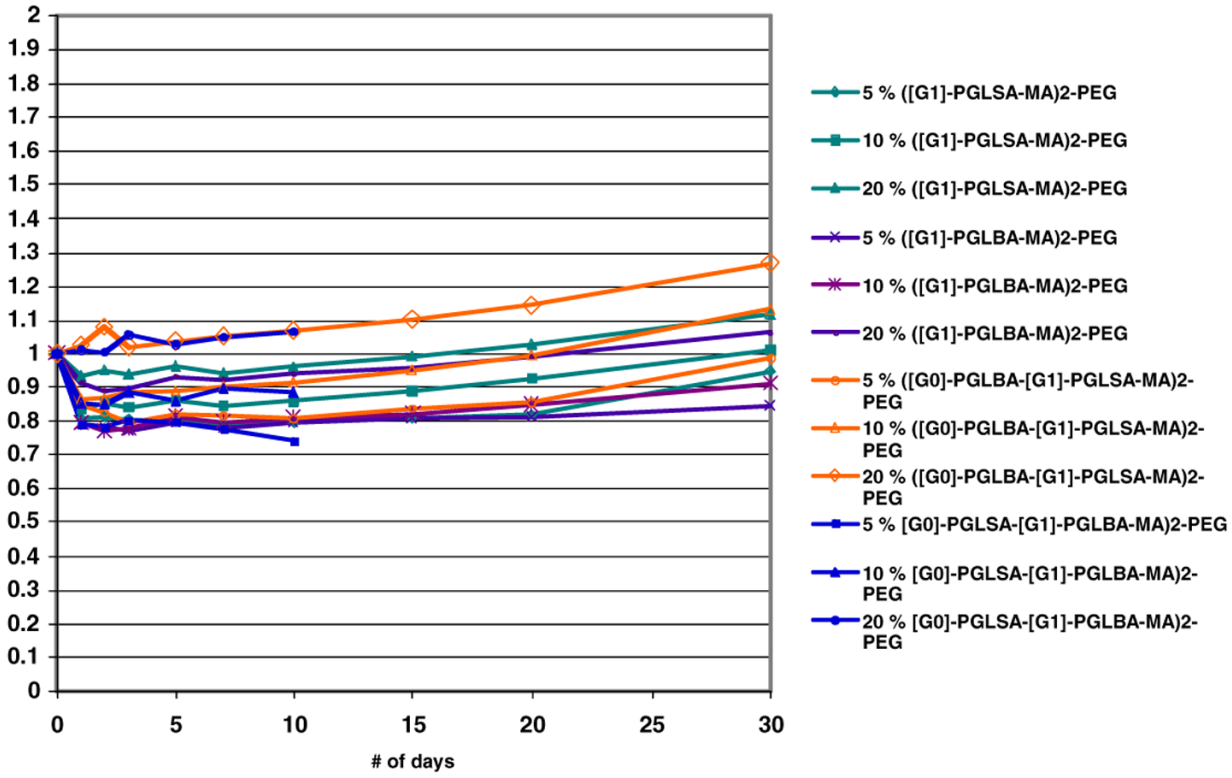

Figure 4.

Normalized weight of the hydrogel samples at 5, 10, and 20% w/v (n = 3), stored in PBS at 37 °C and 5% CO_2 as a function of time. The weight of the sample was taken at the time of polymerization followed by 1, 3, 5, 7, 10, 15, 20, and 30 days thereafter. With the exception of four samples, the gels didn't swell beyond their original weight

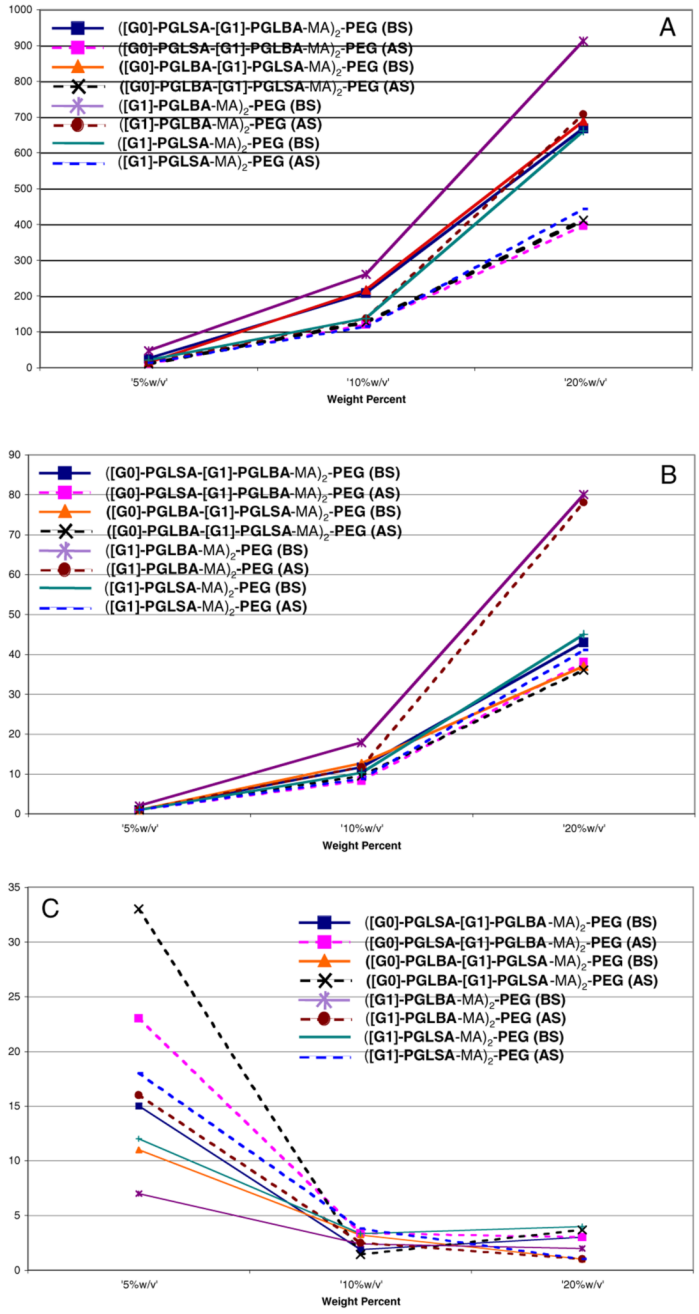

Figure 5.

Mechanical properties, (A) E, (B) |G*|, and (C) δ of the four dendrimer formulations at a range of concentrations (5, 10, and 20 % w/v) before swelling (BS) and after swelling (AS). The |G*| and δ were recorded at a frequency of 1 Hz (n = 3).

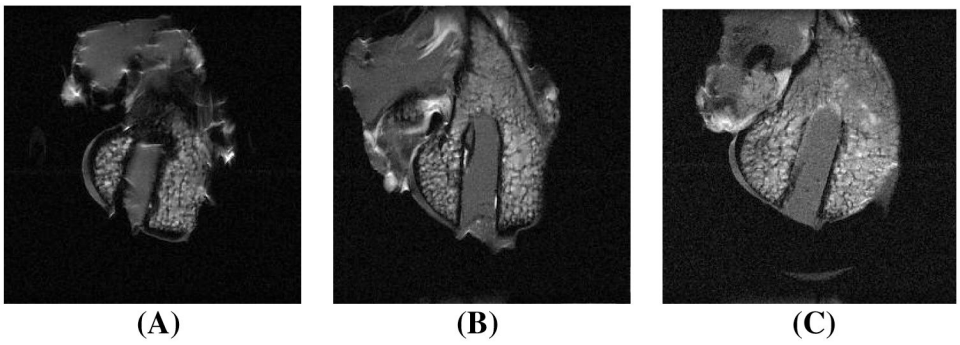

Figure 6.
Sagittal Plane MR image of **(A)** 5, **(B)** 10, and **(C)** 20% w/v of (**[G1]-PGLBA**-MA)$_2$**-PEG** hydrogel completely filling the volume of the defect after repeated loading with a 3 Kg dead-weight.

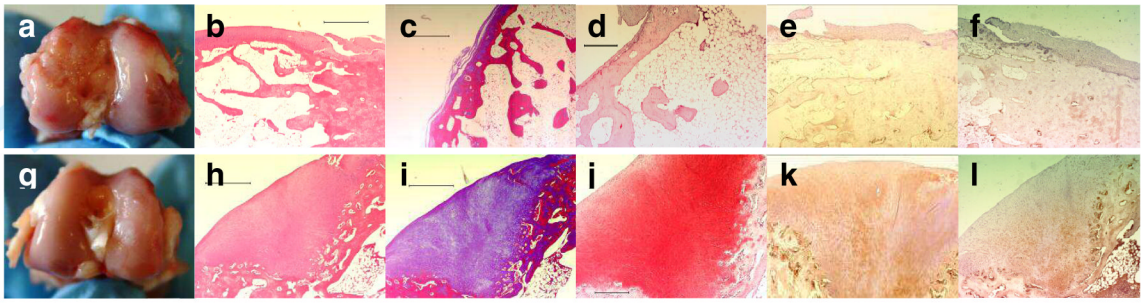

Figure 7.

Histology of untreated (**b–f**) and treated (**h–l**) osteochondral defects. Pictures of the femurs after 24 weeks of healing (**a, g**) showed considerably smoother surfaces for the treated knees. H & E (**b, h**) and Masson's trichrome staining (**c, i**) showed considerable cell infiltration into the wound site for treated knees. Safranin-O staining (**d, j**) showed that only the treated defects displayed any considerable GAG production (GAGs stain red). Immunohistology showed that the ECM in the treated knees had significant collagen production, and that the collagen was primarily type II (**e, k**) and not type I (**f, l**). Scale bar = 100μm.

Table 1

Rheological parameters for all the biodendrimer formulations before swelling SD = ± 1 standard deviation.

	([G0]-PGLSA-[G1]-PGLBA-MA)$_2$-PEG			([G0]-PGLBA-[G1]-PGLSA-MA)$_2$-PEG			([G1]-PGLSA-MA)$_2$-PEG			([G1]-PGLBA-MA)$_2$-PEG		
	5%	**10%**	**20%**	**5%**	**10%**	**20%**	**5%**	**10%**	**20%**	**5%**	**10%**	**20%**
Compressive Modulus (Mean ± SD) kPa	25±3	208±10	668±15	14±2	216±8	688±10	21±2	137±8	661±13	47±1	260±8	912±16
Complex Shear Modulus (Mean ± SD) kPa	1±0.1	12±1	43±1	1±0.1	13±1	37±0.5	1±0.1	10±1	45±3	2±0.1	17.8±1	80±2
Loss Angle (Mean ± SD) degrees	15±1	2±0.4	3±0.1	11±3	3±0.7	1±0.44	12±3	3±0.4	4±1	7±1	2±0.5	2±1

Table 2

Rheological parameters for all the biodendrimer formulations after swelling SD = ± 1 standard deviation.

	([G0]-PGLSA-[G1]-PGLBA-MA)$_2$-PEG			([G0]-PGLBA-[G1]-PGLSA-MA)$_2$-PEG			([G1]-PGLSA-MA)$_2$-PEG			([G1]-PGLBA-MA)$_2$-PEG		
	5%	**10%**	**20%**	**5%**	**10%**	**20%**	**5%**	**10%**	**20%**	**5%**	**10%**	**20%**
Compressive Modulus(Mean ± SD) kPa	10±0.1	120±4	396±34	10±2	127±3	411±16	13±3	114±11	442±10	13±1	137±10	708±14
Complex Shear Modulus(Mean ± SD) kPa	1±0.1	8±0.5	38±2	1±0.1	10±1	36±2	1±0.1	9±1	41±2	1±0.1	12±3	78±1
Loss Angle (Mean ± SD) degrees	23±4	3±0.4	3±1	33±1	1.4±0.4	4±0.2	18±1	4±0.1	1±0.1	16±1	3± 0.7	1±0.1